Chapter 1

Finite Element Volume Method

1.1 Notation for Numerical Grids

We begin by defining the numerical grid in both space and time. We define these grids from a starting location x_0 and a beginning time t^0. For any $j, n \in \mathbb{N}$ we have

$$x_j = x_0 + j\Delta x, \tag{1.1a}$$

$$t^n = t^0 + n\Delta t \tag{1.1b}$$

which produces a uniform grid; x_j in space and t^n in time. The FEVM can be readily adapted to nonuniform grids and we restrict our description of the method to uniform grids for simplicity. We will extend this notation to describe locations and times not on the grid by allowing (1.1) to have subscripts and superscripts in $\mathbb{R}$.

The grid notation naturally extends to our quantities of interest for example for a general quantity q

$$q_j^n = q(x_j, t^n). \tag{1.2}$$

The description of our numerical method focuses on cells which are the regions surrounding the grid points. The j^{th} cell is the region $\left[x_{j-1/2}, x_{j+1/2}\right]$ centred around x_j. For each cell we define the average of a quantity q in that cell as

$$\overline{q}_j = \frac{1}{\Delta x} \int_{x_{j-1/2}}^{x_{j+1/2}} q(x,t)\, dx. \tag{1.3}$$

In the FEVM we reconstruct quantities at various points inside the cell from the cell average values. However, we would like to distinguish between the two reconstructions that are possible at each cell edge, which both exist due to the

overlap of neighbouring cells. To do this we use superscripts so that for the cell edge $x_{j+1/2}$ and a general quantity q, we have $q^-_{j+1/2}$ as the reconstructed value of q at $x_{j+1/2}$ from the j^{th} cell and $q^+_{j+1/2}$ as the reconstructed value of q at $x_{j+1/2}$ from the $(j+1)^{th}$ cell. Since the particular time level is typically obvious from context and hence omitted the use of a superscript will not clutter the notation.

1.2 Structure Overview

To describe the FEVM we first present an overview of the evolution step and then provide the details for each component. We begin our evolution step with all the cell averages for h, w and G at time t^n and all the nodal values of b. We write these as vectors from the 0^{th} cell to the m^{th} in the following way

$$\overline{\boldsymbol{h}} = \begin{bmatrix} \overline{h}^n_0 \\ \overline{h}^n_1 \\ \vdots \\ \overline{h}^n_m \end{bmatrix}, \qquad \overline{\boldsymbol{w}} = \begin{bmatrix} \overline{w}^n_0 \\ \overline{w}^n_1 \\ \vdots \\ \overline{w}^n_m \end{bmatrix}, \qquad \overline{\boldsymbol{G}} = \begin{bmatrix} \overline{G}^n_0 \\ \overline{G}^n_1 \\ \vdots \\ \overline{G}^n_m \end{bmatrix} \qquad \text{and} \qquad \boldsymbol{b} = \begin{bmatrix} b_0 \\ b_1 \\ \vdots \\ b_m \end{bmatrix}.$$

The evolution step proceeds as follows:

(I) Reconstruct the Quantities Inside the Cells: We reconstruct the quantities h, w, G and b inside every cell at various points. The values of h, w and G in the j^{th} cell are reconstructed at $x_{j-1/2}$, x_j and $x_{j+1/2}$ using the reconstruction operators $\mathcal{R}^+_{j-1/2}$, $\mathcal{R}_j$ and $\mathcal{R}^-_{j+1/2}$ respectively. The bed profile b in the j^{th} cell is reconstructed at $x_{j-1/2}$, $x_{j-1/6}$, $x_{j+1/6}$ and $x_{j+1/2}$ using the reconstruction operators $\mathcal{B}_{j-1/2}$, $\mathcal{B}_{j-1/6}$, $\mathcal{B}_{j+1/6}$ and $\mathcal{B}_{j+1/2}$ respectively. So

that

$$\begin{aligned} h^+_{j-1/2} &= \mathcal{R}^+_{j-1/2}\left(\overline{\boldsymbol{h}}\right), & G^+_{j-1/2} &= \mathcal{R}^+_{j-1/2}\left(\overline{\boldsymbol{G}}\right), \\ h_j &= \mathcal{R}_j\left(\overline{\boldsymbol{h}}\right), & G_j &= \mathcal{R}_j\left(\overline{\boldsymbol{G}}\right), \\ h^-_{j+1/2} &= \mathcal{R}^-_{j+1/2}\left(\overline{\boldsymbol{h}}\right), & G^-_{j+1/2} &= \mathcal{R}^-_{j+1/2}\left(\overline{\boldsymbol{G}}\right), \end{aligned}$$

$$\begin{aligned} w^+_{j-1/2} &= \mathcal{R}^+_{j-1/2}\left(\overline{\boldsymbol{w}}\right), & b_{j-1/2} &= \mathcal{B}_{j-1/2}\left(\boldsymbol{b}\right), \\ w_j &= \mathcal{R}_j\left(\overline{\boldsymbol{w}}\right), & b_{j-1/6} &= \mathcal{B}_{j-1/6}\left(\boldsymbol{b}\right), \\ w^-_{j+1/2} &= \mathcal{R}^-_{j+1/2}\left(\overline{\boldsymbol{w}}\right), & b_{j+1/6} &= \mathcal{B}_{j+1/6}\left(\boldsymbol{b}\right), \\ & & b_{j+1/2} &= \mathcal{B}_{j+1/2}\left(\boldsymbol{b}\right). \end{aligned}$$

This generates the vectors of these quantities reconstructed for every cell; $\hat{\boldsymbol{h}}$, $\hat{\boldsymbol{w}}$, $\hat{\boldsymbol{G}}$ and $\hat{\boldsymbol{b}}$ which are

$$\hat{\boldsymbol{h}} = \begin{bmatrix} h^+_{-1/2} \\ h_0 \\ h^-_{1/2} \\ h^+_{1/2} \\ \vdots \\ h_m \\ h^-_{m+1/2} \end{bmatrix}, \quad \hat{\boldsymbol{w}} = \begin{bmatrix} w^+_{-1/2} \\ w_0 \\ w^-_{1/2} \\ w^+_{1/2} \\ \vdots \\ w_m \\ w^-_{m+1/2} \end{bmatrix}, \quad \hat{\boldsymbol{G}} = \begin{bmatrix} G^+_{-1/2} \\ G_0 \\ G^-_{1/2} \\ G^+_{1/2} \\ \vdots \\ G_m \\ G^-_{m+1/2} \end{bmatrix} \quad \text{and} \quad \hat{\boldsymbol{b}} = \begin{bmatrix} b_{-1/2} \\ b_{-1/6} \\ b_{1/6} \\ b_{1/2} \\ \vdots \\ b_{m+1/6} \\ b_{m+1/2} \end{bmatrix}.$$

(II) Calculate the Velocity Over the Domain: The remaining unknown quantity u is calculated by solving the elliptic equation (**??**) with a FEM from which we obtain $u_{j-1/2}$, u_j and $u_{j+1/2}$ for every cell. We denote the solution of the FEM by the map $\mathcal{G}$ taking $\hat{\boldsymbol{h}}$, $\hat{\boldsymbol{G}}$ and $\hat{\boldsymbol{b}}$ as inputs. So that

$$\hat{\boldsymbol{u}} = \begin{bmatrix} u_{-1/2} \\ u_0 \\ u_{1/2} \\ \vdots \\ u_m \\ u_{m+1/2} \end{bmatrix} = \mathcal{G}\left(\hat{\boldsymbol{h}}, \hat{\boldsymbol{G}}, \hat{\boldsymbol{b}}\right).$$

(III) Calculate All the Fluxes Across the Cell Interfaces: We calculate the average fluxes $F_{j-1/2}$ and $F_{j+1/2}$ across the cell boundaries $x_{j-1/2}$ and $x_{j+1/2}$

over time using $\mathcal{F}_{j-1/2}$ and $\mathcal{F}_{j+1/2}$ so that

$$F_{j-1/2} = \mathcal{F}_{j-1/2}\left(\hat{\boldsymbol{h}}, \hat{\boldsymbol{w}}, \hat{\boldsymbol{G}}, \hat{\boldsymbol{b}}, \hat{\boldsymbol{u}}\right),$$
$$F_{j+1/2} = \mathcal{F}_{j+1/2}\left(\hat{\boldsymbol{h}}, \hat{\boldsymbol{w}}, \hat{\boldsymbol{G}}, \hat{\boldsymbol{b}}, \hat{\boldsymbol{u}}\right).$$

(IV) Calculate All the Source Terms for the Cells: We calculate the source term contribution to the cell average of a quantity over a time step S_j with the operator $\mathcal{S}$ like so

$$S_j = \mathcal{S}_j\left(\hat{\boldsymbol{h}}, \hat{\boldsymbol{w}}, \hat{\boldsymbol{b}}, \hat{\boldsymbol{u}}\right).$$

(V) Update All the Cell Averages Using a Forward Euler Approximation: We update the cell average values from time t^n to the next time level combining a fractional step method and a forward Euler approximation for the flux and source terms.

(VI) Update All the Cell Averages Using a Second-Order SSP Runge-Kutta Method: We repeat steps (I)-(V) and use SSP Runge-Kutta time stepping to calculate $\overline{\boldsymbol{h}}$ and $\overline{\boldsymbol{G}}$ at t^{n+1} with second-order accuracy in space and time.

(I) Reconstruct the Quantities Inside the Cells

We now provide the details for how each of the quantities inside the j^{th} cell are calculated. For h, w and G the reconstructions is performed from the cell averages. While b is reconstructed from the nodal values.

(I).1 Reconstruction for h, w and G

We reconstruct h, w and G with piecewise functions that are linear over a cell with discontinuous jumps at the cell edges. Since h, w and G use the same reconstruction operators we will demonstrate them for a general quantity q. For the j^{th} cell we reconstruct the values of q at $x_{j-1/2}$, x_j and $x_{j+1/2}$ in the following way

$$q^+_{j-1/2} = \mathcal{R}^+_{j-1/2}\left(\overline{\boldsymbol{q}}\right) = \bar{q} - \frac{\Delta x}{2} d_j, \tag{1.4a}$$
$$q_j = \mathcal{R}_j\left(\overline{\boldsymbol{q}}\right) = \bar{q}, \tag{1.4b}$$
$$q^-_{j+1/2} = \mathcal{R}^-_{j+1/2}\left(\overline{\boldsymbol{q}}\right) = \bar{q} + \frac{\Delta x}{2} d_j \tag{1.4c}$$

where

$$d_j = \text{minmod}\left(\theta\frac{\overline{q}_j - \overline{q}_{j-1}}{\Delta x}, \frac{\overline{q}_{j+1} - \overline{q}_{j-1}}{2\Delta x}, \theta\frac{\overline{q}_{j+1} - \overline{q}_j}{\Delta x}\right)$$

with $\theta \in [1, 2]$.

Definition 1.1. The minmod function takes a list of $x_j \in \mathbb{R}$. If all elements have the same sign then minmod returns the element with smallest absolute value, otherwise it returns 0.

$$\text{minmod}\left(x_0, x_1, \dots\right) := \begin{cases} \min\left\{x_j\right\} & x_j > 0 \ \forall j \\ \max\left\{x_j\right\} & x_j < 0 \ \forall j \\ 0 & \text{otherwise} \end{cases}.$$

The nonlinear limiting used to calculate d_j ensures that the reconstruction of h, w and G inside the cell does not introduce non-physical oscillations and is thus Total Variation Diminishing (TVD). It does this by reverting the slope d_j to zero near local extrema, resulting in a first-order approximation there which is TVD. Away from local extrema d_j will be the gradient with the smallest absolute value, making our reconstruction second-order accurate. The choice of the θ parameter changes the disspativeness of the reconstruction with $\theta = 1$ being the most disspative and $\theta = 2$ being the least disspative.

The reconstruction operator $\mathcal{R}_j$ is second-order accurate regardless of the presence of local extrema. This can be seen through the error analysis of the midpoint method for which we get that

$$\overline{q} = \frac{1}{\Delta x}\int_{x_{j-1/2}}^{x_{j+1/2}} q \, dx = q_j + \mathcal{O}\left(\Delta x^2\right). \tag{1.5}$$

(I).2 Reconstruction for b

To reconstruct b at $x_{j-1/2}$, $x_{j-1/6}$, $x_{j+1/6}$ and $x_{j+1/2}$ we construct the cubic polynomial $C_j(x)$ centred around x_j

$$C_j(x) = c_0\left(x - x_j\right)^3 + c_1\left(x - x_j\right)^2 + c_2\left(x - x_j\right) + c_3. \tag{1.6}$$

By forcing $C_j(x)$ to pass through the nodal values b_{j-2}, b_{j-1}, b_{j+1} and b_{j+2} we get

$$\begin{bmatrix} -8\Delta x^3 & 4\Delta x^2 & -2\Delta x & 1 \\ -\Delta x^3 & \Delta x^2 & -\Delta x & 1 \\ \Delta x^3 & \Delta x^2 & \Delta x & 1 \\ 8\Delta x^3 & 4\Delta x^2 & 2\Delta x & 1 \end{bmatrix} \begin{bmatrix} c_0 \\ c_1 \\ c_2 \\ c_3 \end{bmatrix} = \begin{bmatrix} b_{j-2} \\ b_{j-1} \\ b_{j+1} \\ b_{j+2} \end{bmatrix}.$$

Solving this we get the polynomial coefficients

$$\begin{aligned} c_0 &= \frac{-b_{j-2} + 2b_{j-1} - 2b_{j+1} + b_{j+2}}{12\Delta x^3}, \\ c_1 &= \frac{b_{j-2} - b_{j-1} - b_{j+1} + b_{j+2}}{6\Delta x^2}, \\ c_2 &= \frac{b_{j-2} - 8b_{j-1} + 8b_{j+1} - b_{j+2}}{12\Delta x}, \\ c_3 &= \frac{-b_{j-2} + 4b_{j-1} + 4b_{j+1} - b_{j+2}}{6}. \end{aligned}$$

We require a bed that is continuous across the cell edges and so on top of the reconstruction of the bed given by these coefficients and (1.6) we also average between the two reconstructions at the cell edge so that

$$b_{j-1/2} = \mathcal{B}_{j-1/2}(\boldsymbol{b}) = \frac{1}{2}\left(C_j(x_{j-1/2}) + C_{j-1}(x_{j-1/2})\right), \tag{1.7a}$$

$$b_{j-1/6} = \mathcal{B}_{j-1/6}(\boldsymbol{b}) = C_j(x_{j-1/6}), \tag{1.7b}$$

$$b_{j+1/6} = \mathcal{B}_{j+1/6}(\boldsymbol{b}) = C_j(x_{j+1/6}), \tag{1.7c}$$

$$b_{j+1/2} = \mathcal{B}_{j+1/2}(\boldsymbol{b}) = \frac{1}{2}\left(C_j(x_{j+1/2}) + C_{j+1}(x_{j+1/2})\right). \tag{1.7d}$$

(II) Calculate the Velocity Over the Domain

The elliptic equation that relates the conserved variables h and G and the bed profile b to the primitive variable u was given in Def **??**. To form the FEM we take the weak form of Def **??** which is

$$\int_\Omega Gv\,dx = \int_\Omega uh\left(1 + \frac{\partial h}{\partial x}\frac{\partial b}{\partial x} + \frac{1}{2}h\frac{\partial^2 b}{\partial x^2} + \frac{\partial b}{\partial x}^2\right) - \frac{\partial}{\partial x}\left(\frac{1}{3}h^3\frac{\partial u}{\partial x}\right)v\,dx.$$

Using integration by parts and assuming Dirichlet boundary conditions we get

$$\begin{aligned} \int_\Omega Gv\,dx = \int_\Omega uh\left(1 + \frac{\partial b}{\partial x}^2\right)v\,dx + \int_\Omega \frac{1}{3}h^3\frac{\partial u}{\partial x}\frac{\partial v}{\partial x}\,dx \\ - \int_\Omega \frac{1}{2}h^2\frac{\partial b}{\partial x}u\frac{\partial v}{\partial x}\,dx. - \int_\Omega \frac{1}{2}h^2\frac{\partial b}{\partial x}\frac{\partial u}{\partial x}v\,dx. \end{aligned} \tag{1.8}$$

This weak formulation implies that if G and h are members of the function space $\mathbb{L}^p$ and b is a member of the Sobolev space $\mathbb{W}^{1,p}$ then u is a member of the

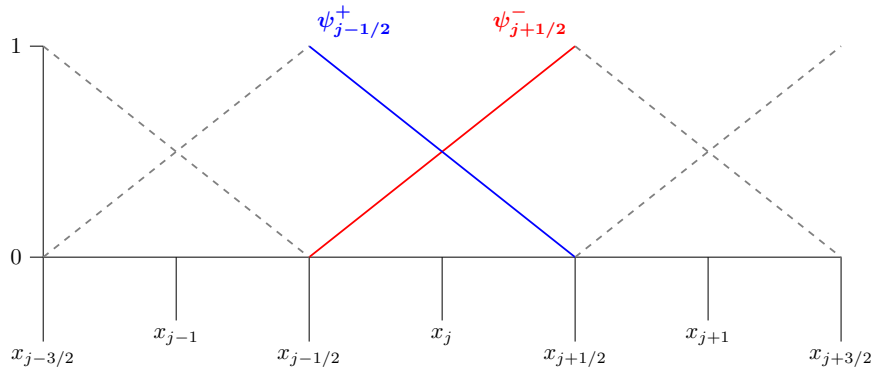

Figure 1.1: Basis functions for discontinuous linear elements.

Sobolev space $\mathbb{W}^{1,p}$ as well. Since our method requires the derivative of u to be well defined and hence that $u \in \mathbb{W}^{1,p}$ we will restrict ourselves to only allow $h, G \in \mathbb{L}^p$ and $b \in \mathbb{W}^{1,p}$.

We simplify (1.8) by performing the integration over the cells and then summing the integrals together to get the equation for the entire domain

$$\sum_j \int_{x_{j-1/2}}^{x_{j+1/2}} \left[\left(uh\left(1 + \frac{\partial b}{\partial x}^2\right) - \frac{1}{2}h^2 \frac{\partial b}{\partial x}\frac{\partial u}{\partial x} - G \right) v + \left(\frac{1}{3}h^3 \frac{\partial u}{\partial x} - \frac{1}{2}h^2 \frac{\partial b}{\partial x} u \right) \frac{\partial v}{\partial x} \right] dx = 0 \quad (1.9)$$

which holds for all test functions v. The next step is to replace the functions for the quantities h, G, b and u with their basis function approximations.

(II).1 Basis Function Approximations

For h and G we use the basis functions ψ which are linear inside a cell and 0 everywhere outside the cell as shown in Figure 1.1. This produces a second-order approximation to h and G inside the cell and allows for discontinuities at the cell edges. Since these basis functions are in $\mathbb{L}^p$ our basis function approximations to h and G are in the appropriate function space.

From the basis functions ψ we have the following representation for h and G in our finite element method

$$h = \sum_j h^+_{j-1/2}\psi^+_{j-1/2} + h^-_{j+1/2}\psi^-_{j+1/2}, \quad (1.10a)$$

$$G = \sum_j G^+_{j-1/2}\psi^+_{j-1/2} + G^-_{j+1/2}\psi^-_{j+1/2}. \quad (1.10b)$$

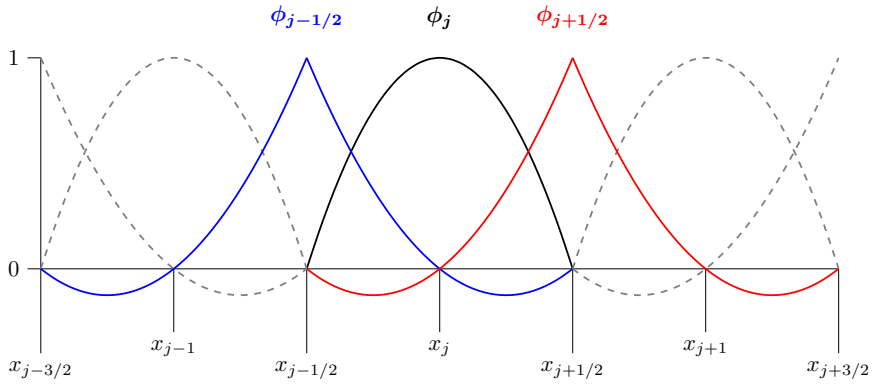

Figure 1.2: Basis functions for continuous piecewise quadratic elements.

For u we require a locally calculated second-order approximation to the first derivative, which forces at least a quadratic representation of u in each cell. Since we require u to be a member of $\mathbb{W}^{1,p}$, u will be continuous. Therefore, we use basis functions ϕ that are continuous at the cell edges, resulting in the basis functions depicted in Figure 1.2.

From the basis functions ϕ our basis function approximation to u is

$$u = \sum_j u_{j-1/2}\phi_{j-1/2} + u_j\phi_j + u_{j+1/2}\phi_{j+1/2}. \tag{1.11}$$

For the bed term we require a local approximation to the second derivative of the bed that is second-order accurate. To allow for an appropriate second derivative of the bed profile, b must be a member of $\mathbb{W}^{2,p}$ which is smoother than indicated by the elliptic equation (1.8). We choose the cubic basis functions γ which are continuous across the cell edges, as the bed profile must be continuous. These basis functions are shown in Figure 1.3 and from them we get our basis function approximation to b

$$b = \sum_j b_{j-1/2}\gamma_{j-1/2} + b_{j-1/6}\gamma_{j-1/6} + b_{j+1/6}\gamma_{j+1/6} + b_{j+1/2}\gamma_{j+1/2}. \tag{1.12}$$

With $b_{j-1/2}$ and $b_{j+1/2}$ being well defined as our method (1.7) forces both reconstructions at the cell edges to be the same.

(II).2 Calculation of Element-wise Matrices

The integral equation (1.9) holds for all v. However, since our solution space has the basis functions ϕ it is sufficient to satisfy (1.9) for all ϕ to generate the

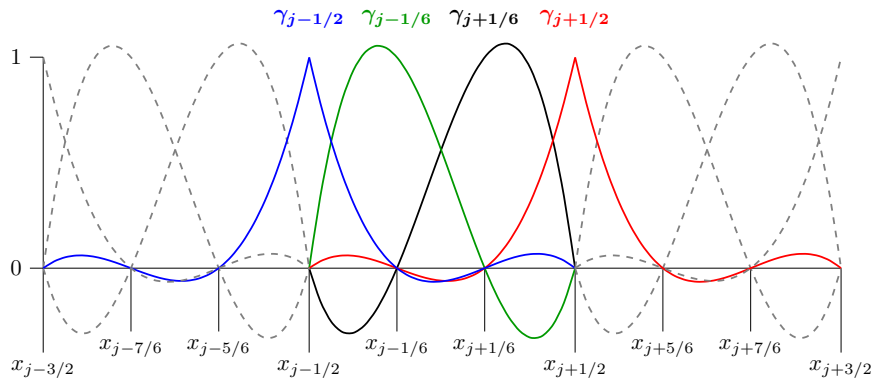

Figure 1.3: Basis functions for continuous piecewise cubic elements.

solution. Since only the basis functions $\phi_{j-1/2}$, ϕ_j and $\phi_{j+1/2}$ are non-zero over the j^{th} cell we can calculate the j^{th} term in the sum (1.9) like so

$$\int_{x_{j-1/2}}^{x_{j+1/2}} \left[\left(uh\left(1+\frac{\partial b}{\partial x}^2\right) - \frac{1}{2}h^2\frac{\partial b}{\partial x}\frac{\partial u}{\partial x} - G \right) \begin{bmatrix} \phi_{j-1/2} \\ \phi_j \\ \phi_{j+1/2} \end{bmatrix} + \left(\frac{1}{3}h^3\frac{\partial u}{\partial x} - \frac{1}{2}h^2\frac{\partial b}{\partial x}u\right)\frac{\partial}{\partial x}\left(\begin{bmatrix} \phi_{j-1/2} \\ \phi_j \\ \phi_{j+1/2} \end{bmatrix}\right) \right] dx \quad (1.13)$$

where we use our finite element approximations for h (1.10a), G (1.10b), u (1.11) and b (1.12). Because the basis functions over an element are just translations of the the other basis functions, this integral can be generalised by moving to the ξ space. The mapping from the x space to the ξ space is

$$x = x_j + \xi\frac{\Delta x}{2}.$$

Making the change of variables from x to ξ in (1.13) we get

$$\frac{\Delta x}{2}\int_{-1}^{1} \left[\left(uh\left(1+\frac{4}{\Delta x^2}\frac{\partial b}{\partial \xi}^2\right) - \frac{2}{\Delta x^2}h^2\frac{\partial b}{\partial \xi}\frac{\partial u}{\partial \xi} - G \right) \begin{bmatrix} \phi_{j-1/2} \\ \phi_j \\ \phi_{j+1/2} \end{bmatrix} + \frac{4}{\Delta x^2}\left(\frac{1}{3}h^3\frac{\partial u}{\partial \xi} - \frac{1}{2}h^2\frac{\partial b}{\partial \xi}u\right)\frac{\partial}{\partial \xi}\left(\begin{bmatrix} \phi_{j-1/2} \\ \phi_j \\ \phi_{j+1/2} \end{bmatrix}\right) \right] d\xi.$$

We will demonstrate the rest of the process for the uh term as an example

and then give the remaining integrals in the Appendix[]. The uh term is

$$\frac{\Delta x}{2}\int_{-1}^{1} uh \begin{bmatrix}\phi_{j-1/2}\\ \phi_j \\ \phi_{j+1/2}\end{bmatrix} d\xi.$$

Since the integral is computed over $\left[x_{j-1/2}, x_{j+1/2}\right]$, there are only a few non-zero contributions from the finite element approximations to h and u, so we have

$$\begin{aligned}
&\frac{\Delta x}{2}\int_{-1}^{1} \left(u_{j-1/2}\phi_{j-1/2} + u_j\phi_j + u_{j+1/2}\phi_{j+1/2}\right) \\
&\qquad \left(h^+_{j-1/2}\psi^+_{j-1/2} + h^-_{j+1/2}\psi^-_{j+1/2}\right) \begin{bmatrix}\phi_{j-1/2}\\ \phi_j \\ \phi_{j+1/2}\end{bmatrix} d\xi \\
&= \frac{\Delta x}{2}\left(h^+_{j-1/2}\int_{-1}^{1} \psi^+_{j-1/2} \begin{bmatrix} \phi_{j-1/2}\phi_{j-1/2} & \phi_j\phi_{j-1/2} & \phi_{j+1/2}\phi_{j-1/2} \\ \phi_{j-1/2}\phi_j & \phi_j\phi_j & \phi_{j+1/2}\phi_j \\ \phi_{j+1/2}\phi_{j-1/2} & \phi_{j+1/2}\phi_j & \phi_{j+1/2}\phi_{j+1/2}\end{bmatrix} d\xi \right. \\
&\quad \left. + h^-_{j+1/2}\int_{-1}^{1} \psi^-_{j+1/2} \begin{bmatrix} \phi_{j-1/2}\phi_{j-1/2} & \phi_j\phi_{j-1/2} & \phi_{j+1/2}\phi_{j-1/2} \\ \phi_{j-1/2}\phi_j & \phi_j\phi_j & \phi_{j+1/2}\phi_j \\ \phi_{j+1/2}\phi_{j-1/2} & \phi_{j+1/2}\phi_j & \phi_{j+1/2}\phi_{j+1/2}\end{bmatrix} d\xi \right) \\
&\qquad \begin{bmatrix}u_{j-1/2}\\ u_j \\ u_{j+1/2}\end{bmatrix}.
\end{aligned}$$

Calculating the integrals of all the basis function combinations we get

$$\begin{aligned}
&\frac{\Delta x}{2}\int_{-1}^{1} uh \begin{bmatrix}\phi_{j-1/2}\\ \phi_j \\ \phi_{j+1/2}\end{bmatrix} d\xi = \\
&\quad \frac{\Delta x}{2}\begin{bmatrix} \frac{7}{30}h^+_{j-1/2} + \frac{1}{30}h^-_{j+1/2} & \frac{4}{30}h^+_{j-1/2} & -\frac{1}{30}h^+_{j-1/2} - \frac{1}{30}h^-_{j+1/2} \\ \frac{4}{30}h^+_{j-1/2} & \frac{16}{30}h^+_{j-1/2} + \frac{16}{30}h^-_{j+1/2} & \frac{4}{30}h^-_{j+1/2} \\ -\frac{1}{30}h^+_{j-1/2} - \frac{1}{30}h^-_{j+1/2} & \frac{4}{30}h^-_{j+1/2} & \frac{1}{30}h^+_{j-1/2} + \frac{7}{30}h^-_{j+1/2}\end{bmatrix} \\
&\qquad \begin{bmatrix}u_{j-1/2}\\ u_j \\ u_{j+1/2}\end{bmatrix}. \quad (1.14)
\end{aligned}$$

(II).3 Assembly of the Global Matrix

By combining all the matrices generated by the integral of each of the u terms we get the j^{th} cells contribution to the stiffness matrix $\mathbf{A}_j$. Likewise all the integrals of the remaining term Gv generate the vector $\boldsymbol{g}_j$. Therefore, (1.9) can be rewritten as

$$\sum_j \mathbf{A}_j \begin{bmatrix} u_{j-1/2} \\ u_j \\ u_{j+1/2}. \end{bmatrix} = \sum_j \boldsymbol{g}_j. \tag{1.15}$$

This is a penta-diagonal matrix equation which can be solved by standard banded matrix solution techniques to obtain

$$\hat{\boldsymbol{u}} = \mathcal{G}\left(\hat{\boldsymbol{h}}, \hat{\boldsymbol{G}}, \hat{\boldsymbol{b}}\right) = \mathbf{A}^{-1}\boldsymbol{g} \tag{1.16}$$

as desired.

(III) Calculate All the Fluxes Across the Cell Interfaces

We use Kurganovs method [5] to calculate the flux across a cell interface. This method was employed because; it can handle discontinuities across the cell boundary and only requires an estimate of the maximum and minimum wave speeds. This is precisely the situation for the Serre equations which do not have an expression for the characteristics but do possess estimates on the maximum and minimum wave speeds (**??**).

We will only demonstrate the calculation of the flux term for $F_{j+1/2}$ as the process to calculate the flux term $F_{j-1/2}$ is identical but with different cells. For a general quantity q, Kurganov's method [5] is

$$F_{j+\frac{1}{2}} = \frac{a^+_{j+\frac{1}{2}} f\left(q^-_{j+\frac{1}{2}}\right) - a^-_{j+\frac{1}{2}} f\left(q^+_{j+\frac{1}{2}}\right)}{a^+_{j+\frac{1}{2}} - a^-_{j+\frac{1}{2}}} + \frac{a^+_{j+\frac{1}{2}} a^-_{j+\frac{1}{2}}}{a^+_{j+\frac{1}{2}} - a^-_{j+\frac{1}{2}}} \left[q^+_{j+\frac{1}{2}} - q^-_{j+\frac{1}{2}}\right] \tag{1.17}$$

where $a^+_{j+\frac{1}{2}}$ and $a^-_{j+\frac{1}{2}}$ are given by the wave speed bounds. For the Serre equations we have the wave speed bounds (**??**) and so we obtain

$$a^-_{j+\frac{1}{2}} = \min\left\{0\ ,\ u^-_{j+1/2} - \sqrt{gh^-_{j+1/2}}\ ,\ u^+_{j+1/2} - \sqrt{gh^+_{j+1/2}}\right\}, \tag{1.18}$$

$$a^+_{j+\frac{1}{2}} = \max\left\{0\ ,\ u^-_{j+1/2} + \sqrt{gh^-_{j+1/2}}\ ,\ u^+_{j+1/2} + \sqrt{gh^+_{j+1/2}}\right\}. \tag{1.19}$$

The flux functions $f(q^-_{j+\frac{1}{2}})$ and $f(q^+_{j+\frac{1}{2}})$ are evaluated using the reconstructed values from the j^{th} and $(j+1)^{th}$ cell respectively. From the continuity equation (**??**) we have

$$f\left(h^-_{j+\frac{1}{2}}\right) = u^-_{j+1/2} h^-_{j+1/2},$$
$$f\left(h^+_{j+\frac{1}{2}}\right) = u^+_{j+1/2} h^+_{j+1/2}.$$

For the irrotationality equation (**??**) we have

$$\begin{aligned} f\left(G^-_{j+\frac{1}{2}}\right) &= u^-_{j+1/2} G^-_{j+1/2} + \frac{g}{2}\left(h^-_{j+1/2}\right)^2 - \frac{2}{3}\left(h^-_{j+1/2}\right)^3 \left[\left(\frac{\partial u}{\partial x}\right)^-_{j+1/2}\right]^2 \\ &\quad + \left(h^-_{j+1/2}\right)^2 u^-_{j+1/2} \left(\frac{\partial u}{\partial x}\right)^-_{j+1/2} \left(\frac{\partial b}{\partial x}\right)^-_{j+1/2}, \\ f\left(G^+_{j+\frac{1}{2}}\right) &= u^+_{j+1/2} G^+_{j+1/2} + \frac{g}{2}\left(h^+_{j+1/2}\right)^2 - \frac{2}{3}\left(h^+_{j+1/2}\right)^3 \left[\left(\frac{\partial u}{\partial x}\right)^+_{j+1/2}\right]^2 \\ &\quad + \left(h^+_{j+1/2}\right)^2 u^+_{j+1/2} \left(\frac{\partial u}{\partial x}\right)^+_{j+1/2} \left(\frac{\partial b}{\partial x}\right)^+_{j+1/2}. \end{aligned}$$

During the reconstruction process we calculated $h^+_{j-1/2}$, $h^-_{j+1/2}$, $G^+_{j-1/2}$, $G^-_{j+1/2}$ (1.4) while during the calculation of velocity we obtained $u^\pm_{j+1/2} = u_{j+1/2}$; as u is continuous across the cell boundaries. Therefore, we further require an approximation to $\left(\frac{\partial b}{\partial x}\right)^\pm_{j+1/2}$ and $\left(\frac{\partial u}{\partial x}\right)^\pm_{j+1/2}$ to calculate the flux (1.17).

(III).1 Calculation of Derivatives

To calculate the derivatives in u and b we use the basis function approximation to these quantities in the FEM. For u we have the quadratic $P^u_j(x)$ that passes through $u_{j-1/2}$, u_j and $u_{j+1/2}$ while for b we have the cubic $P^b_j(x)$ that passes through $b_{j-1/2}$, $b_{j-1/6}$, $b_{j+1/6}$ and $b_{j+1/2}$. So we have

$$P^u_j(x) = p^u_0 (x - x_j)^2 + p^u_1 (x - x_j) + p^u_2, \tag{1.20a}$$
$$P^b_j(x) = p^b_0 (x - x_j)^3 + p^b_1 (x - x_j)^2 + p^b_2 (x - x_j) + p^b_3, \tag{1.20b}$$

By forcing the polynomials to pass through these reconstructed values we get that for $P_j^u(x)$

$$\begin{aligned} p_0^u &= \frac{u_{j-1/2} - 2u_j + u_{j+1/2}}{2\Delta x^2}, \\ p_1^u &= \frac{-u_{j-1/2} + u_{j+1/2}}{\Delta x}, \\ p_2^u &= u_j. \end{aligned}$$

While for $P_j^b(x)$ we get

$$\begin{aligned} p_0^b &= \frac{-9b_{j-1/2} + 27b_{j-1/6} - 27b_{j+1/6} + 9b_{j+1/2}}{2\Delta x^3}, \\ p_0^b &= \frac{9b_{j-1/2} - 9b_{j-1/6} - 9b_{j+1/6} + 9b_{j+1/2}}{4\Delta x^2}, \\ p_0^b &= \frac{b_{j-1/2} - 27b_{j-1/6} + 27b_{j+1/6} - b_{j+1/2}}{8\Delta x}, \\ p_0^b &= \frac{-b_{j-1/2} + 9b_{j-1/6} + 9b_{j+1/6} - b_{j+1/2}}{16}. \end{aligned}$$

Taking the derivative of the polynomials (1.20) we get

$$\begin{aligned} \frac{\partial}{\partial x} P_j^u(x) &= 2p_0^u \left(x - x_j\right) + p_1^u, \\ \frac{\partial}{\partial x} P_j^b(x) &= 3p_0^b \left(x - x_j\right)^2 + 2p_1^b \left(x - x_j\right) + p_2^b. \end{aligned}$$

This gives a second-order approximation to the derivative of u and b at $x_{j+1/2}$ based on the j^{th} cell, the process for the $(j+1)^{th}$ cell is the same and we get

$$\left(\frac{\partial u}{\partial x}\right)^-_{j+1/2} = \frac{\partial}{\partial x} P_j^u(x_{j+1/2}) \tag{1.21a}$$

$$\left(\frac{\partial u}{\partial x}\right)^+_{j+1/2} = \frac{\partial}{\partial x} P_{j+1}^u(x_{j+1/2}) \tag{1.21b}$$

$$\left(\frac{\partial b}{\partial x}\right)^-_{j+1/2} = \frac{\partial}{\partial x} P_j^b(x_{j+1/2}) \tag{1.21c}$$

$$\left(\frac{\partial b}{\partial x}\right)^+_{j+1/2} = \frac{\partial}{\partial x} P_{j+1}^b(x_{j+1/2}) \tag{1.21d}$$

Therefore we possess all the terms need to calculate the approximation to the flux (1.17) for both the continuity and irrotationality equation, as desired. However, we must make a slight modification to ensure that our scheme is well balanced and recovers the lake at rest steady state solution.

(III).2 Modification to h to Enforce Well Balancing

To recover the lake at rest steady state solution we follow the work of Audusse et al. [1], who accomplished this for the Shallow Water Wave equations. It was demonstrated that this process could also be extended to the Serre equations [7]. To enforce well balancing h is modified at the cell edges in the following way; we first calculate

$$\dot{b}^-_{j+1/2} = w^-_{j+1/2} - h^-_{j+1/2} \qquad \text{and} \qquad \dot{b}^+_{j+1/2} = w^+_{j+1/2} - h^+_{j+1/2}. \tag{1.22}$$

Find the maximum

$$\grave{b}_{j+1/2} = \max\left\{\dot{b}^-_{j+1/2}, \dot{b}^+_{j+1/2}\right\}$$

then we define

$$\grave{h}^-_{j+1/2} = \max\left\{0, w^-_{j+1/2} - \grave{b}_{j+1/2}\right\}, \tag{1.23a}$$

$$\grave{h}^+_{j+1/2} = \max\left\{0, w^+_{j+1/2} - \grave{b}_{j+1/2}\right\}. \tag{1.23b}$$

We use $\grave{h}^-_{j+1/2}$ and $\grave{h}^+_{j+1/2}$ instead of $h^-_{j+1/2}$ and $h^+_{j+1/2}$ to calculate the flux term $F_{j+1/2}$ in (1.17) for both the continuity (**??**) and irrotationality (**??**) equation.

Applying the same process but with different cells we obtain $F_{j-1/2}$ and we have

$$F_{j-1/2} = \mathcal{F}_{j-1/2}\left(\hat{\boldsymbol{h}}, \hat{\boldsymbol{w}}, \hat{\boldsymbol{G}}, \hat{\boldsymbol{b}}, \hat{\boldsymbol{u}}\right), \tag{1.24a}$$

$$F_{j+1/2} = \mathcal{F}_{j+1/2}\left(\hat{\boldsymbol{h}}, \hat{\boldsymbol{w}}, \hat{\boldsymbol{G}}, \hat{\boldsymbol{b}}, \hat{\boldsymbol{u}}\right) \tag{1.24b}$$

for both the continuity and irrotationality equation as desired.

(IV) Calculate All the Source Terms for the Cells

The Serre equations in conservation law form (**??**) contain a flux term and a source term, to treat this numerically we use a first-order splitting method. This requires an approximation to the source term at the cell centre x_j which we denote as S_j. Since the continuity equation (**??**) has no source term, we will just present the calculation of the source term for the irrotationality equation (**??**).

Following the work of Audusse et al. [1], we split our approximation to S_j into the centred source term S_{ci} and the corrective interface source terms $S^-_{j+\frac{1}{2}}$ and $S^+_{j+\frac{1}{2}}$. Where S_{ci} is the naive source term approximation and $S^-_{j+\frac{1}{2}}$ and $S^+_{j+\frac{1}{2}}$ are

artificial terms that ensure that the flux and source term cancel properly for the lake at rest steady state.

We calculate the centred source term using

$$S_{ci} = -\frac{1}{2}\left(h_j\right)^2 u_j \left(\frac{\partial u}{\partial x}\right)_j \left(\frac{\partial^2 b}{\partial x^2}\right)_j + h_j \left(u_j\right)^2 \left(\frac{\partial b}{\partial x}\right)_j \left(\frac{\partial^2 b}{\partial x^2}\right)_j - g h_j \left(\frac{\partial b}{\partial x}\right)_j.$$

Where we use h_j from the reconstruction process (1.4) and u_j from the solution of the elliptic equation (1.16). To calculate the derivatives we employ our polynomial representations of u and b inside a cell. However, to ensure that the terms cancel properly for a lake at rest we must modify our approximation to $\dfrac{\partial b}{\partial x}$ to use $\dot{b}^-_{j+1/2}$ and $\dot{b}^+_{j+1/2}$ from (1.22). Therefore, the following approximations are used in the calculation of S_{ci}

$$\left(\frac{\partial u}{\partial x}\right)_j = \frac{\partial}{\partial x} P^u_j(x_j), \tag{1.25a}$$

$$\left(\frac{\partial b}{\partial x}\right)_j = \frac{\dot{b}^-_{j+1/2} - \dot{b}^+_{j-1/2}}{\Delta x}, \tag{1.25b}$$

$$\left(\frac{\partial^2 b}{\partial x^2}\right)_j = \frac{\partial^2}{\partial x^2} P^b_j(x_j). \tag{1.25c}$$

The corrective interface source terms are

$$S^-_{j+\frac{1}{2}} = \frac{g}{2}\left(\grave{h}^-_{j+\frac{1}{2}}\right)^2 - \frac{g}{2}\left(h^-_{j+\frac{1}{2}}\right)^2,$$
$$S^+_{j-\frac{1}{2}} = \frac{g}{2}\left(h^+_{j-\frac{1}{2}}\right)^2 - \frac{g}{2}\left(\grave{h}^+_{j-\frac{1}{2}}\right)^2.$$

Which makes use of $h^-_{j+\frac{1}{2}}$ and $h^+_{j+\frac{1}{2}}$ obtained from the reconstruction (1.4) and the modified values $\grave{h}^-_{j+\frac{1}{2}}$ and $\grave{h}^+_{j+\frac{1}{2}}$ from (1.23). Combining the centred and interface source terms our approximation to the source term for the irrotationality equation is

$$S_j = \mathcal{S}_j\left(\hat{\boldsymbol{h}}, \hat{\boldsymbol{w}}, \hat{\boldsymbol{b}}, \hat{\boldsymbol{u}}\right) = S^-_{j+\frac{1}{2}} + \Delta x S_{ci} + S^+_{j-\frac{1}{2}}. \tag{1.26}$$

(V) Update All the Cell Averages Using a Forward Euler Approximation

We employ a fractional step method [] to split the flux term and source term part of the Serre equations in conservation law form (**??**). This results in the following

time-stepping method that is first-order accurate in time

$$\overline{q}'_j = \overline{q}^n_j + \frac{\Delta t}{\Delta x}\left(F_{j+\frac{1}{2}} - F_{j-\frac{1}{2}}\right),$$
$$\overline{q}^{n+1}_j = \overline{q}'_j + \frac{\Delta t}{\Delta x} S_j$$

where $F_{j+\frac{1}{2}}$, $F_{j-\frac{1}{2}}$ and S_j are all calculated using the quantities at time t^n. Therefore, this method can be condensed into

$$\overline{q}^{n+1}_j = \overline{q}^n_j + \frac{\Delta t}{\Delta x}\left(F_{j+\frac{1}{2}} - F_{j-\frac{1}{2}} + S_j\right). \tag{1.27}$$

(VI) Update All the Cell Averages Using a Second-Order SSP Runge-Kutta Method

To increase the order of accuracy in time we employ the strong stability preserving Runge-Kutta method [4] to convexly combine multiple first-order time steps (1.27) in the following way

$$\overline{q}'_j = \overline{q}^n_j + \frac{\Delta t}{\Delta x}\left(F_{j+\frac{1}{2}} - F_{j-\frac{1}{2}} + S_j\right), \tag{1.28a}$$
$$\overline{q}''_j = \overline{q}'_j + \frac{\Delta t}{\Delta x}\left(F'_{j+\frac{1}{2}} - F'_{j-\frac{1}{2}} + S'_j\right), \tag{1.28b}$$
$$\overline{q}^{n+1}_j = \frac{1}{2}\left(\overline{q}^n_j + \overline{q}''_j\right). \tag{1.28c}$$

Where we write $F'_{j+\frac{1}{2}}$, $F'_{j-\frac{1}{2}}$ and S'_j to highlight that these terms are calculated using the quantities after the first time step. This results in a time stepping method that preserves the stability of the first-order method (1.27) and is second-order accurate in time. Since all the spatial approximations are second-order accurate the steps (I-VI) result in a complete second-order accurate FEVM for the Serre equations as desired.

1.7 CFL condition

To ensure the stability of our FEVM we use the Courant-Friedrichs-Lewy condition [2] which is necessary for stability. The CFL condition ensures that time steps are small enough so that information is only transferred between neighbouring cells. For the Serre equations the CFL condition is

$$\Delta t \leq \frac{Cr}{\max_j \left\{a^{\pm}_{j+1/2}\right\}} \Delta x \tag{1.29}$$

where $a^{\pm}_{j+1/2}$ are the wavespeed bounds used in Kurganovs flux approximation (1.19) and $0 \leq Cr \leq 1$ is the Courant number. Typically, we use the conservative $Cr = 0.5$ for our numerical experiments.

1.8 Boundary Conditions

To numerically model the Serre equations over finite spatial domains we must enforce boundary conditions at the left and right edge of the domain; $x_{-1/2}$ and $x_{m+1/2}$ respectively. We have only developed Dirichlet boundary conditions for the FEVM, which we enforce using ghost cells located outside the domain boundaries. These ghost cells contain the complete representation of their respective quantities over the cell. For h, w, G and u only one ghost cell at each boundary is required, while for b we require two ghost cells at each boundary. We therefore have ghost cells with the following associated quantities

$$\hat{\boldsymbol{h}}_{-1} = \begin{bmatrix} h^+_{-3/2} \\ h_{-1} \\ h^-_{-1/2} \end{bmatrix}, \qquad \hat{\boldsymbol{h}}_{m+1} = \begin{bmatrix} h^+_{m+1/2} \\ h_{m+1} \\ h^-_{m+3/2} \end{bmatrix},$$

$$\hat{\boldsymbol{w}}_{-1} = \begin{bmatrix} w^+_{-3/2} \\ w_{-1} \\ w^-_{-1/2} \end{bmatrix}, \qquad \hat{\boldsymbol{w}}_{m+1} = \begin{bmatrix} w^+_{m+1/2} \\ w_{m+1} \\ w^-_{m+3/2} \end{bmatrix},$$

$$\hat{\boldsymbol{G}}_{-1} = \begin{bmatrix} G^+_{-3/2} \\ G_{-1} \\ G^-_{-1/2} \end{bmatrix}, \qquad \hat{\boldsymbol{G}}_{m+1} = \begin{bmatrix} G^+_{m+1/2} \\ G_{m+1} \\ G^-_{m+3/2} \end{bmatrix},$$

$$\hat{\boldsymbol{u}}_{-1} = \begin{bmatrix} u_{-3/2} \\ u_{-1} \\ u_{-1/2} \end{bmatrix}, \qquad \hat{\boldsymbol{u}}_{m+1} = \begin{bmatrix} u_{m+1/2} \\ u_{m+1} \\ u_{m+3/2} \end{bmatrix}$$

$$\hat{\boldsymbol{b}}_{-2} = \begin{bmatrix} b_{-5/2} \\ b_{-13/6} \\ b_{-11/6} \\ b_{-3/2} \end{bmatrix}, \quad \hat{\boldsymbol{b}}_{-1} = \begin{bmatrix} b_{-3/2} \\ b_{-7/6} \\ b_{-5/6} \\ b_{-1/2} \end{bmatrix}, \quad \hat{\boldsymbol{b}}_{m+1} = \begin{bmatrix} b_{m+1/2} \\ b_{m+5/6} \\ b_{m+7/6} \\ b_{m+3/2} \end{bmatrix}, \quad \hat{\boldsymbol{b}}_{m+2} = \begin{bmatrix} b_{m+3/2} \\ b_{m+11/6} \\ b_{m+13/6} \\ b_{m+5/2} \end{bmatrix}.$$

To ensure that the solution of u by (1.16) agrees with the boundary conditions $\hat{\boldsymbol{u}}_{-1}$ and $\hat{\boldsymbol{u}}_m$ the element matrices $\mathbf{A}_0$ and $\mathbf{A}_m$ and vectors $\boldsymbol{g}_0$ and $\boldsymbol{g}_m$ must be modified in the following way

$$\mathbf{A}_0 = \begin{bmatrix} 1 & 0 & 0 \\ a_{21} & a_{22} & a_{23} \\ a_{31} & a_{32} & a_{33} \end{bmatrix}, \qquad \boldsymbol{g}_0 = \begin{bmatrix} u_{-1/2} \\ g_1 \\ g_2 \end{bmatrix}, \tag{1.30}$$

$$\mathbf{A}_m = \begin{bmatrix} a_{11} & a_{12} & a_{13} \\ a_{21} & a_{22} & a_{23} \\ 0 & 0 & 1 \end{bmatrix}, \qquad \boldsymbol{g}_m = \begin{bmatrix} g_0 \\ g_1 \\ u_{m+1/2} \end{bmatrix}. \tag{1.31}$$

These are then combined with the other element contributions to the global matrix as in (1.15).

1.9 Dry Beds

Dry beds are handled adequately by all steps of our FEVM in their current form, except the FEM solution for u. For the FEM a dry bed presents two issues; when $h = 0$ the stiffness matrix will become singular, and when h is small u may become quite large.

In previous work [9] we employed direct banded matrix solvers such as the Thomas algorithm to solve (1.16), however such methods rely on non-singular matrices and so are unsuitable for dry beds. To deal with this an LU decomposition algorithm by Press et al. [8] was used. This algorithm solves banded matrix problems using an LU decomposition with partial pivoting, which inserts small non-zero pivots when their value is below some tolerance value p_{tol}. It does this while also keeping the banded matrix structure, and so is not as memory intensive as a standard LU decomposition. This results in a FEM that could allow for $h = 0$, but still faced the problem of large u values when h was small.

To deal with large u values we restricted our solution of the FEM for u to cells where $\overline{h}_j > h_{tol}$ and modified our approximation to $h^+_{j-1/2}$ and $h^-_{j+1/2}$ in our stiffness matrix. To restrict the domain of our solution we search through the domain at the beginning of each first-order step and identify wet regions where $\overline{h}_j \geq h_{tol}$ and dry regions where $\overline{h}_j < h_{tol}$. In the dry regions we set h, G and u to be zero uniformly over the cell. In the wet regions we solve the FEM with the appropriate boundary conditions and the following modifications to $h^+_{j-1/2}$ and $h^-_{j+1/2}$

$$h^+_{j-1/2} = h^+_{j-1/2} + \frac{h_{base}}{h^+_{j-1/2}}, \tag{1.32a}$$

$$h^-_{j+1/2} = h^-_{j+1/2} + \frac{h_{base}}{h^-_{j+1/2}}. \tag{1.32b}$$

Where on the right hand side we mean $h^+_{j-1/2}$ and $h^-_{j+1/2}$ as calculated from the reconstruction (1.4). This modification ensures that as $h \to 0$ then $u \to 0$ by increasing the size of h in the stiffness matrix.

Typically we had $p_{tol} = 10^{-20}$, $h_{tol} = 10^{-8}$ and $h_{base} = 10^{-4}$ which allowed for an accurate calculation of u in the presence of dry beds and very small water depths.

Chapter 2

Validation

2.1 Analytic Validation

2.1.1 Soliton

2.1.2 Lake at Rest

2.2 Forced Solution Validation

2.2.1 Travelling Gaussian

$$h(x,t) = a_0 + a_1 \exp\left(-\frac{((x - a_2 t) - a_3)^2}{2a_4}\right) \tag{2.1}$$

$$u(x,t) = a_5 \exp\left(-\frac{((x - a_2 t) - a_3)^2}{2a_4}\right) \tag{2.2}$$

$$b(x) = a_6 \sin(a_7 x) \tag{2.3}$$

2.3 Experimental Validation

2.3.1 Beji

2.3.2 Synolakis

2.3.3 Roeber

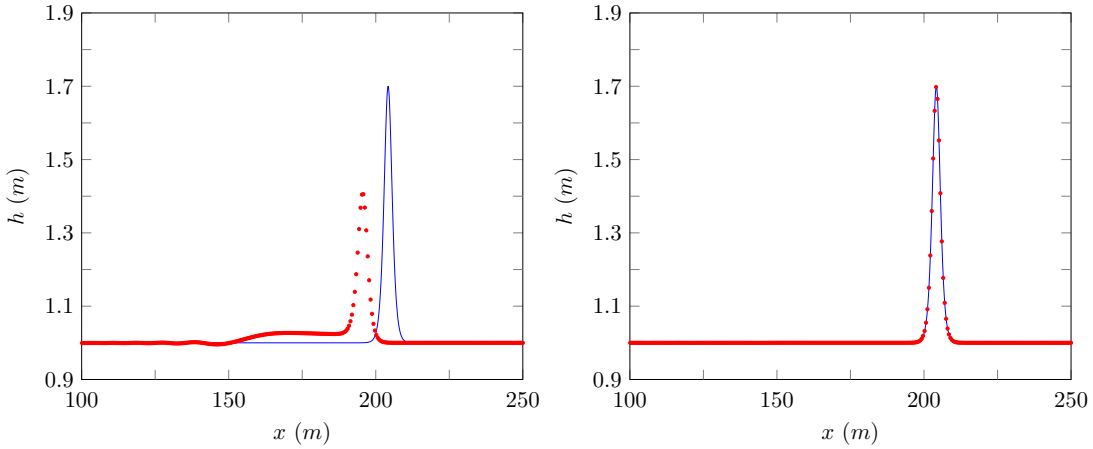

(a) FDVM_1

(b) FDVM_2

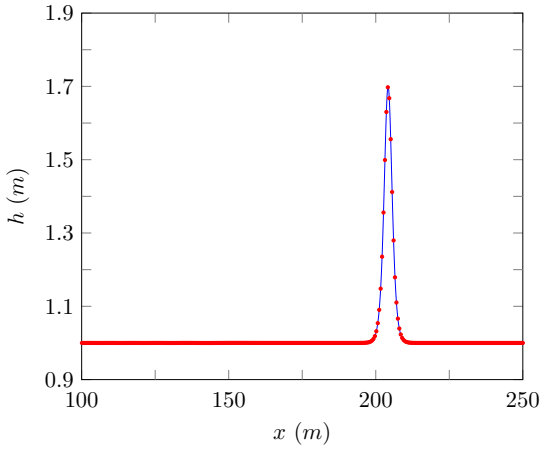

(c) FEVM_2

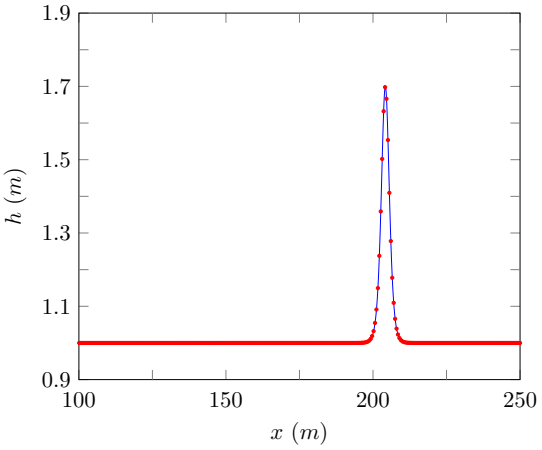

(d) FDVM_3

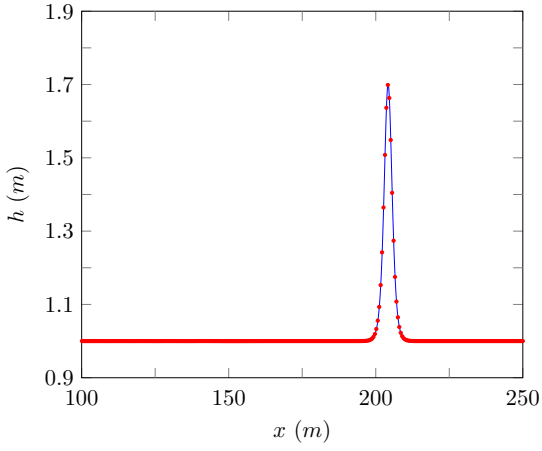

(e) $\mathcal{D}$

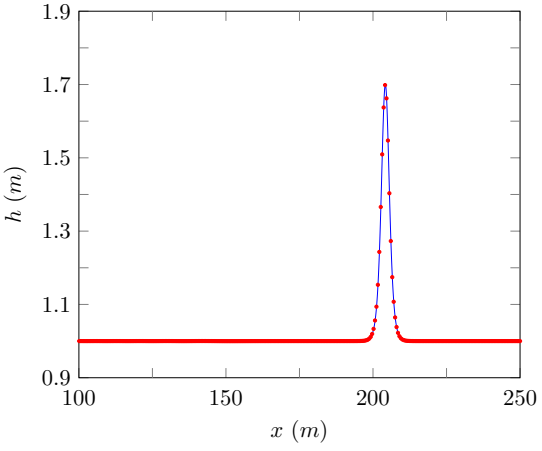

(f) $\mathcal{W}$

Figure 2.1: Comparison of the analytic solution (–) and numerical solution with $\Delta x = 100/2^{11} m$ (•) for the soliton problem at $t = 50s$ for all methods.

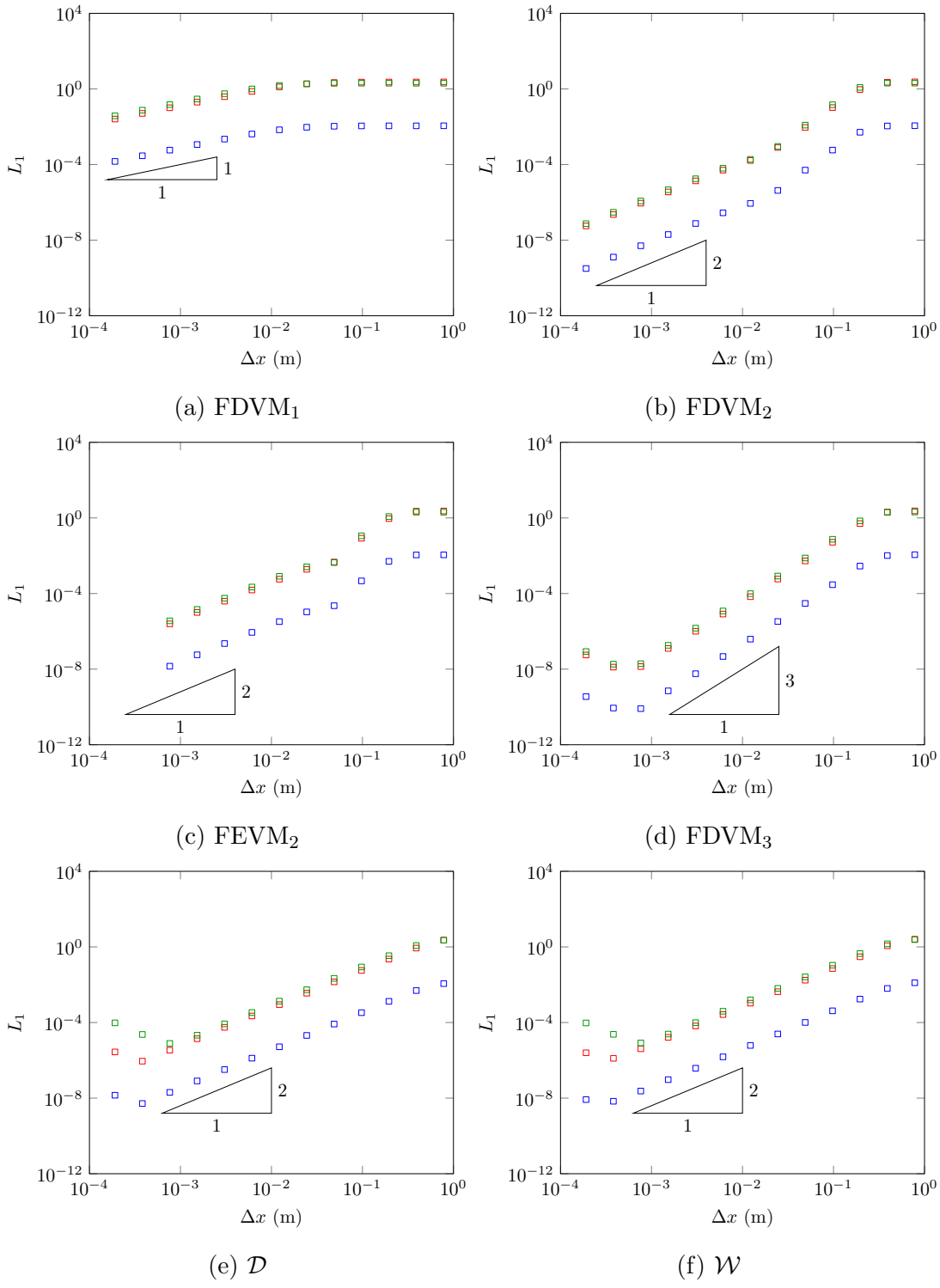

(a) FDVM_1 (b) FDVM_2

(c) FEVM_2 (d) FDVM_3

(e) $\mathcal{D}$ (f) $\mathcal{W}$

Figure 2.2: Convergence plots as measured by the L_1 norm for h (□), u (□) and G (□) for the soliton problem for all methods.

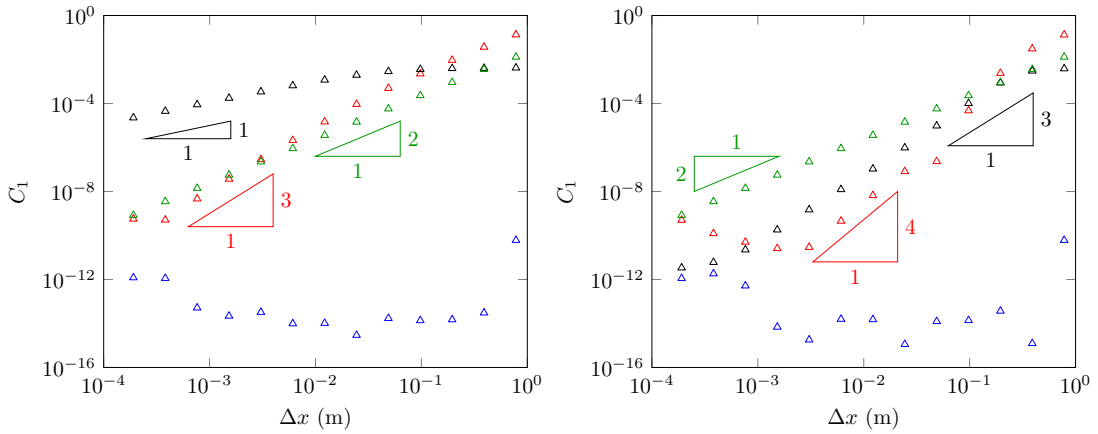

(a) FDVM$_1$

(b) FDVM$_2$

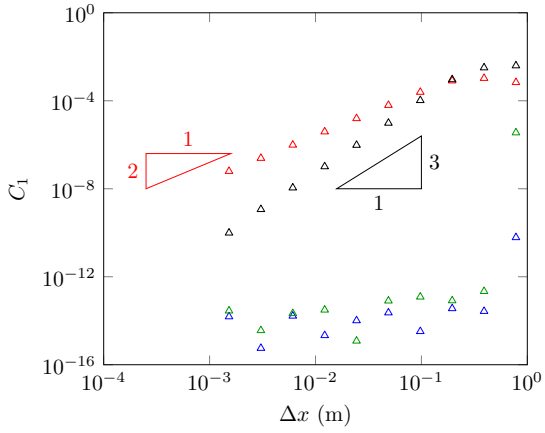

(c) FEVM$_2$

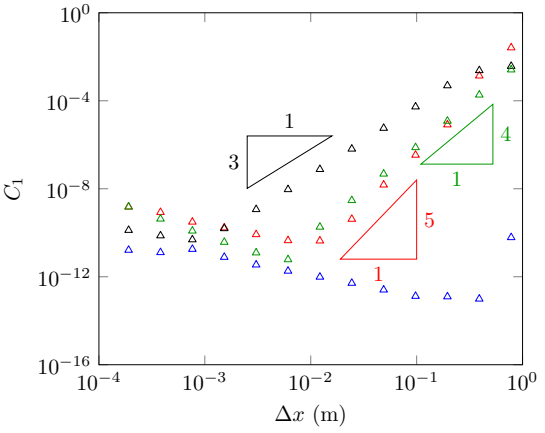

(d) FDVM$_3$

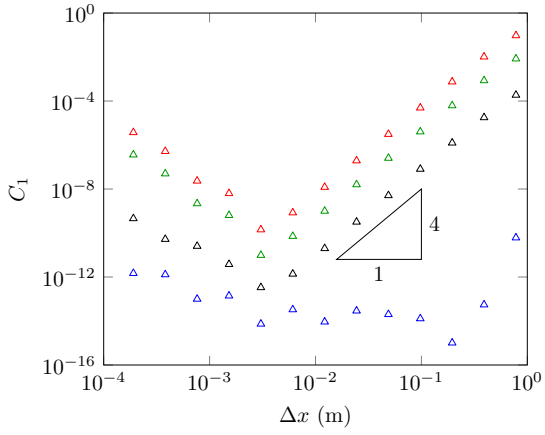

(e) $\mathcal{D}$

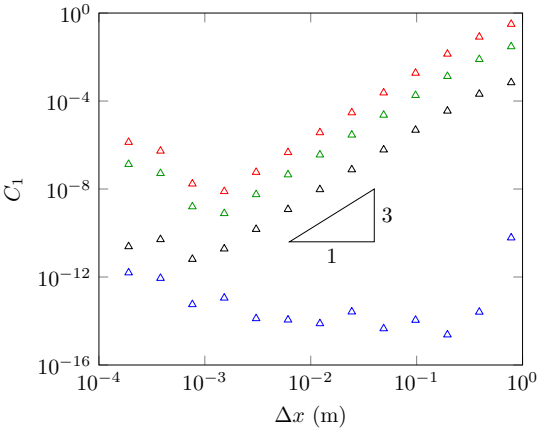

(f) $\mathcal{W}$

Figure 2.3: Conservation plots as measured by C_1 for h (△), uh (△), G (△) and $\mathcal{H}$ (△) for the soliton problem for all methods.

Bibliography

[1] Emmanuel Audusse, François Bouchut, Marie-Odile Bristeau, Rupert Klein, and Benoît Perthame. A fast and stable well–balanced scheme with hydrostatic reconstruction for shallow water flows. *SIAM Journal on Scientific Computing*, 25(6):2050–2065, 2004.

[2] Richard Courant, Kurt Friedrichs, and Hans Lewy. On the partial difference equations of mathematical physics. *IBM journal of Research and Development*, 11(2):215–234, 1967.

[3] A. G. Filippini, M. Kazolea, and M. Ricchiuto. A flexible genuinely nonlinear approach for nonlinear wave propagation, breaking and run-up. *Journal of Computational Physics*, 310:381–417, 2016.

[4] Sigal Gottlieb, Chi-Wang Shu, and Eitan Tadmor. Strong stability-preserving high-order time discretization methods. *SIAM review*, 43(1):89–112, 2001.

[5] A. Kurganov, S. Noelle, and G. Petrova. Semidiscrete central-upwind schemes for hyperbolic conservation laws and Hamilton-Jacobi equations. *Journal of Scientific Computing, Society for Industrial and Applied Mathematics*, 23(3): 707–740, 2002.

[6] Peter D Lax and Robert D Richtmyer. Survey of the stability of linear finite difference equations. *Communications on pure and applied mathematics*, 9(2): 267–293, 1956.

[7] Jordan Pitt. A second order well balanced hybrid finite volume and finite difference method for the serre equations, 2014.

[8] William H Press, Saul A Teukolsky, William T Vetterling, and Brian P Flannery. *Numerical recipes in C*, volume 2. Cambridge university press, 1996.

[9] C. Zoppou, J. Pitt, and S. Roberts. Numerical solution of the fully non-linear weakly dispersive serre equations for steep gradient flows. *Applied Mathematical Modelling*, 48:70–95, 2017.